

## EXTENDED IR EMISSION AT PROXIMITY OF RED GIANTS

T. Le Bertre<sup>1</sup>, F. Boulanger<sup>2</sup>, G. Lagache<sup>2</sup>, N. Mauron<sup>3</sup>, F.-X. Désert<sup>4</sup>, N. Epchtein<sup>5</sup>,  
P. Le Sidaner<sup>1</sup>

<sup>1</sup>UMR 8540. Observatoire de Paris. Paris. France

<sup>2</sup>IAS. Orsay. France

<sup>3</sup>ISTEEM. Montpellier. France

<sup>4</sup>Observatoire de Grenoble. Grenoble. France

<sup>5</sup>Observatoire de la Côte d'Azur. Département Fresnel. Nice. France

### ABSTRACT

Images at 60 and 90  $\mu\text{m}$  of  $7' \times 7'$  fields centered at proximity of luminous red giants with known distances have been acquired with ISOPHOT. The data show gradients of emission towards the positions of the red giants. In some cases we detect isolated sources of emission, probably due to blobs of interstellar matter heated to  $\sim 25\text{--}40\text{ K}$  by the nearby red giant. This particular situation allows to characterize these blobs. We find sizes in the range 0.1–0.5 pc and masses in dust in the range  $10^{-5}\text{--}10^{-3} M_{\odot}$ .

Key words: AGB stars; circumstellar shells; dust; interstellar matter; ISOPHOT.

### 1. INTRODUCTION

Miras are luminous red giants with luminosities around  $10^4 L_{\odot}$ . They are variable and follow a period-luminosity relation which allows to determine their distances. They may undergo mass loss at rates as large as a few  $10^{-5} M_{\odot} \text{ yr}^{-1}$ . Thus, they can be surrounded by circumstellar shells which extend to large distances, up to  $\sim 1\text{ pc}$ , before dissolving into the interstellar medium (ISM). In fact, the extent of these shells depends on the rate of mass loss, its duration, and on the density of the surrounding ISM, all of these being time and space dependent.

The central stars are so luminous that they can heat dust up to distances  $\sim 1\text{ pc}$ , in these regions which correspond to the external parts of the circumstellar shells and the surrounding ISM. Typically the dust at distances in the range 0.1–1 pc of a  $10^4 L_{\odot}$  red giant reaches a temperature between 20 and 50 K (Le Sidaner & Le Bertre 1996). This has to be compared to the temperature of dust in equilibrium with the interstellar radiation field (ISRF),  $\sim 18\text{ K}$  (Désert et al. 1990).

A few such sources are found in the Solar Neighbourhood within the range 100–1000 pc. To study their

surroundings requires a spatial resolution of around  $1'$  in the wavelength range 50–200  $\mu\text{m}$ . The Infrared Space Observatory (ISO) with the PHOT C100 array was therefore perfectly suited to study the far environment of AGB stars.

### 2. OBSERVATIONS

For this study we requested images at 60 (C\_60 filter) and 90  $\mu\text{m}$  (C\_90) with the C100 array ( $3 \times 3$  detectors). The fields were selected at proximity of well studied sources. To minimize detector drifts, the red giant stars were kept outside the fields. The mapping was done with a  $3 \times 3$  raster without overlap (AOT: PHT22), so that the final images have  $9 \times 9$  pixels. Each image consists of 9 sub-images and the exposure time for these sub-images was 128 seconds. Each image was immediately preceded and followed by an observation of the Fine Calibration Source (FCS) of 32 seconds with the same detector setting and the same filter. The level of the FCS was adjusted by the ISO SOC (Science Operations Centre) to fit the expected maximum astronomical signal. This internal source provides an absolute calibration of the individual C100 detector responses to an accuracy of 18% (Schulz et al. 1999). The 60 and 90  $\mu\text{m}$  images were acquired in sequence so that they overlay exactly. For each field the total time, including overheads, was 3268 seconds (TDT, Target Dedicated Time).

### 3. DATA PROCESSING

The data processing has been done using PIA (Gabriel & Acosta-Pulido 1999 and references therein). For the data presented here we have used the version 8.0 with the latest calibration tables obtained at the ISO Data Centre (IDC).

The C100 detectors were extremely sensitive to cosmic rays and jumps between successive read-outs (glitches) can be observed. Strong ones are followed by a period of a few seconds of variable detector response. All data are affected, but especially those

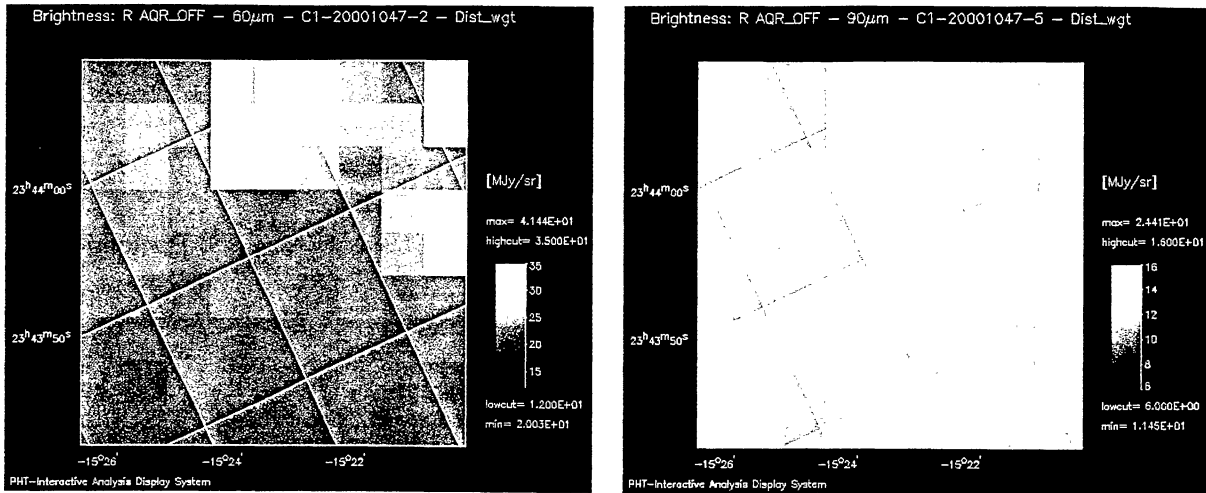


Figure 1. **Left panel:** Field near R Aqr at  $60\mu\text{m}$ ; the rotation angle w.r.t. celestial coordinates (2000.0) is  $64^{\circ}.7$ . North is to the upper right corner and East, to the upper left one. At 215 pc, the pixel corresponds to  $0.047$  pc. The heating source is outside the map, near the upper part of the right superior edge. **Right panel:** Same, but at  $90\mu\text{m}$ .

taken near perigee (orbital phase  $< 0.2$  and  $> 0.8$ ). These effects are handled within PIA at respectively the ERD (Edited Raw Data; 2 Threshold deglitching) and SRD (Signal per Ramp Data; Deglitching) levels.

A drift of the detector response on a longer time scale (several minutes) can also be observed when comparing outputs from the FCSs bracketting each map. This dependence is believed to be a product of the history of the flux received by each detector. It is presently handled with a time interpolation between the 2 FCSs.

The long term behaviour of the detectors do not allow the use of an independent flat field correction. It is then necessary to extract the flat field from the data. This has been done by considering the sub-images where the flux appears uniform. A correction was then derived by comparing the median signal of each individual pixel to the median of the 9 pixel signals. This method gives satisfactory results only if at least 5 sub-images can be used. In PIA, the method called the First Quartile normalisation gives results which are comparable. However, for the images where the sky background presents a gradient across the complete field, these methods cannot be applied. A new flat fielding method based on a minimization algorithm is being developed by C. Gabriel at IDC to handle these cases and appears promising.

In Figures 1 to 3 we present our results for 3 fields which could be processed as explained above and which are discussed in the following Section. These fields are selected because they offer the most interesting examples of extended emission that we have presently. The present results differ from what we have reported previously (Le Bertre et al. 1998,

1999a, 1999b) due to the use of improved processing algorithms (e.g. 2 Threshold glitch recognition instead of Single Threshold, etc.; see Gabriel & Acosta-Pulido 1999) and updated calibration tables (ibidem) in PIA. Nevertheless, we want to express that the differences bear on the absolute level of the fluxes and not on the structures detected in the images.

#### 4. DISCUSSION

The 3 fields presented here were obtained at proximity of O-rich Miras whose luminosities ( $L$ ) and mass loss rates ( $\dot{M}$ ) have been derived by Le Sidaner & Le Bertre (1996) allowing for the distances ( $d$ ) determined by Le Bertre & Winters (1998). These quantities are reported in Table 1 as well as the distances to the galactic plane ( $z$ ).

In all 3 cases a strong emission is noted in the part of the field which is the nearest to the star. This emission is most probably due to the circumstellar shells. Further away, one finds a peak of emission clearly detached from the previous one. These peaks reveal the presence of blobs of material located at distances in the range  $0.3$ – $1.5$  pc from the central source. The distances,  $d(\text{star}, \text{blob})$ , given in Table 1 assume that the blob and the red giant are in a plane perpendicular to the line of sight. With the spatial resolution of PHOT these blobs are just resolved. Their sizes were estimated from the width of the emission. However, from the appearance of the one detected near NML Tau (Figure 3), one may suspect that they are structured at smaller scales.

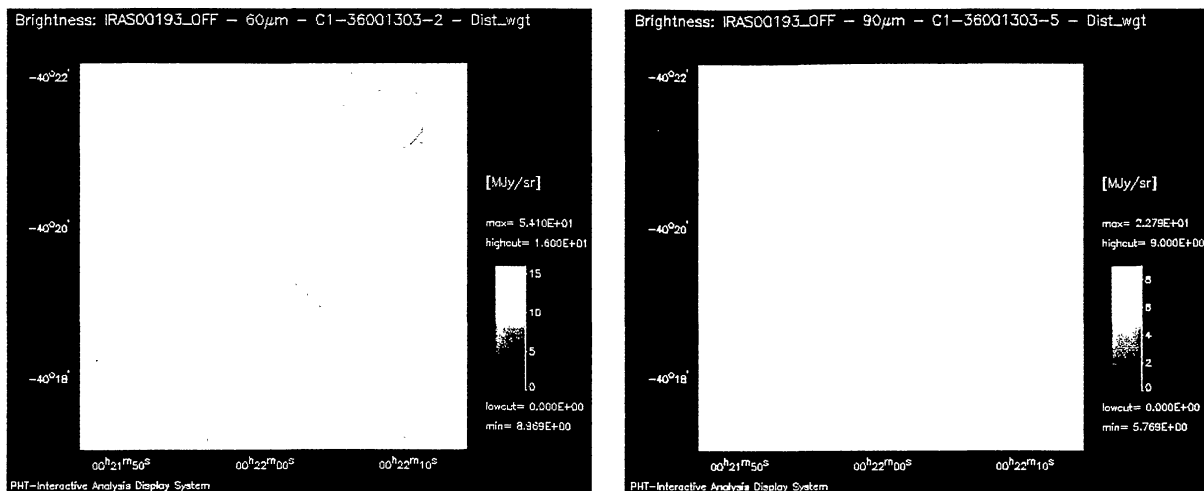


Figure 2. **Left panel:** Field near IRAS00193-4033 (= BE Phe) at  $60\mu\text{m}$ ; the rotation angle w.r.t. celestial coordinates is  $222^\circ 1$ . North is to the lower left corner and East, to the lower right one. At 1680 pc, the pixel corresponds to 0.37 pc. The heating source is outside the map, near the lower left corner. **Right panel:** Same, but at  $90\mu\text{m}$ .

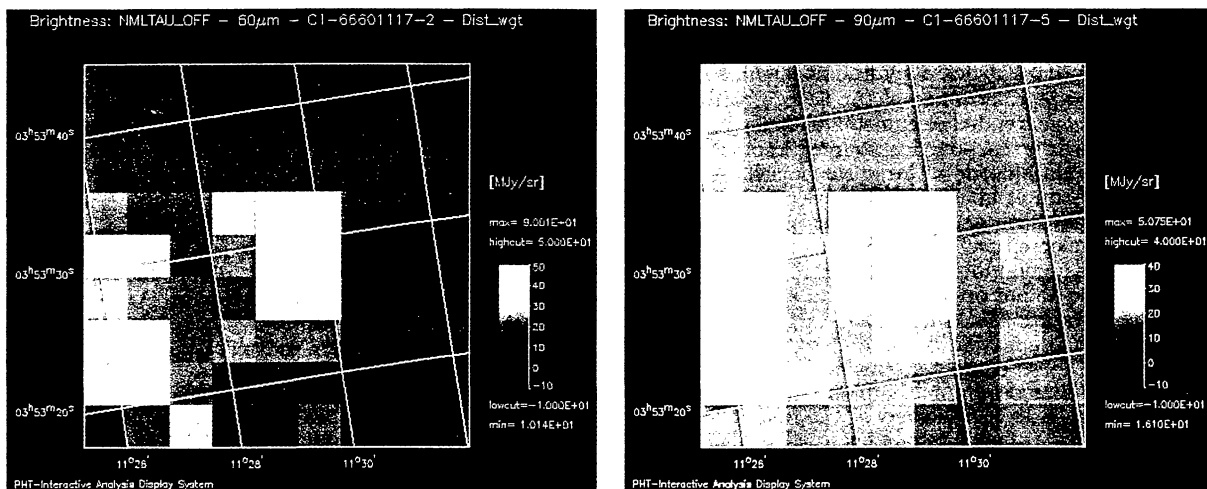


Figure 3. **Left panel:** Field near NML Tau (= IK Tau) at  $60\mu\text{m}$ ; the rotation angle w.r.t. celestial coordinates is  $81^\circ 1$ . North is to the lower left corner and East, to the lower right one. At 245 pc, the pixel corresponds to 0.054 pc. The heating source is outside the map, near the lower part of the left edge. **Right panel:** Same, but at  $90\mu\text{m}$ .

Using the characteristics of the central sources and assuming that the dust is in radiative equilibrium, a temperature  $T_{\text{dust}}$  can be estimated. Then, from the fluxes in the maps, the quantities of dust in the blobs are derived at 60,  $m_{\text{dust}}(60)$ , and at 90  $\mu\text{m}$ ,  $m_{\text{dust}}(90)$ . For these estimates we have adopted

the same dust model (“astronomical” silicate) as Le Sidaner & Le Bertre (1996) did in their modeling of the circumstellar shells.

The former is systematically larger than the latter. In the case of the blob near IRAS 00193 the discrepancy

Table 1. Characteristics of the central sources and of the detected blobs

central sources	$d$ (pc)	$L$ ( $10^3 L_{\odot}$ )	$\dot{M}$ ( $M_{\odot} \text{ yr}^{-1}$ )	$z$ (pc)	$d(\text{star. blob})$ (pc)	size (pc)	$T_{\text{dust}}$ (K)	$m_{\text{dust}}(60)$ ( $M_{\odot}$ )	$m_{\text{dust}}(90)$ ( $M_{\odot}$ )
R Aqr	215	8.0	$1.7 \cdot 10^{-7}$	200	0.27	0.1	40	$3.8 \cdot 10^{-5}$	$1.0 \cdot 10^{-5}$
IRAS 00193	1680	14.0	$9.1 \cdot 10^{-6}$	1625	1.3	0.5	25	$2.7 \cdot 10^{-2}$	$2.9 \cdot 10^{-3}$
NML Tau	245	9.7	$3.2 \cdot 10^{-6}$	130	0.36	0.15	35	$3.6 \cdot 10^{-1}$	$1.5 \cdot 10^{-4}$

reaches almost a factor 10. The temperature that we have adopted assumes that the blob and the heating source are in the plane of the sky. Therefore it might be overestimated and the discrepancy could still be larger. We are obliged to conclude that the optical properties of the dust in these blobs are different from those of the dust in the circumstellar shells.

A possibility is that these blobs contain very small grains (VSG) as those invoked by Désert et al. (1990) to explain the  $60 \mu\text{m}$  excess observed in the ISM spectrum. These VSGs are excited by UV photons and radiate out of equilibrium. They are probably of carbon composition. If this interpretation is correct, then, as the central sources are oxygen-rich, these blobs are certainly of interstellar origin. Also in this context, only  $m_{\text{dust}}(90)$  would have a sense. Adopting these values and a gas-to-dust mass ratio of 100, we get average densities  $n_{\text{H}} \sim 100\text{--}400 \text{ cm}^{-3}$ .

In another programme carried out with ISO, Izumiura & Hashimoto (1999) detected extended shells around some AGB stars. For instance, around the star U Ant ( $d = 256 \text{ pc}$ ), they find at  $90 \mu\text{m}$  a circular emission, extending up to  $4'$  (or  $0.3 \text{ pc}$ ), which they ascribe to an extended circumstellar shell. They have selected nearby carbon-rich sources known to have undergone an episode of large-rate mass loss in the past (Olofsson et al. 1996). Our selection of heating sources was more general without such preference. We only selected well studied sources for which we could have a good model. The emissions that we discussed here do not present a circular symmetry w.r.t. the central star. Also, there is a clear gap between the blob and the emission attributed to the circumstellar shell. These characteristics do not point toward a circumstellar origin for the blobs that are revealed in our data.

## 5. CONCLUSIONS

Extended emission at proximity of AGB stars has been detected by ISO at  $60$  and  $90 \mu\text{m}$ . We find blobs of sizes in the range  $0.1\text{--}0.5 \text{ pc}$  and masses in dust in the range  $10^{-5}\text{--}10^{-3} M_{\odot}$ . In one case, such a blob has been detected at  $1.6 \text{ kpc}$  from the galactic plane. It is noteworthy that this kind of objects, although not directly related to the central sources, will contribute to the point-source fluxes measured by IRAS at  $60$  and  $100 \mu\text{m}$  without sign of contamination in the data.

In the other fields observed by ISO for our programme we have also evidences for such objects, but the full exploitation of the data is still limited by the

present-state processing of the maps. New promising solutions to the flat-fielding problem have been proposed at this conference. Furthermore, a modeling of the behaviour of the C100 detectors under variable illumination, such as the one developed by Coulais & Abergel (1999) for the LW ISOCAM detectors, would allow a better treatment of the data affected by a drift in the responses.

## ACKNOWLEDGMENTS

TL is grateful to C. Gabriel, R. Laureijs and B. Schulz for many rewarding discussions. The data have been processed at IDC (Vilspa) and at the Saclay ISO Centre. This work is supported by the CNRS through the PCMI and ASPS programmes.

## REFERENCES

- Coulais, A., Abergel, A., 1999, Proc. "The Universe as seen by ISO", P. Cox & M. Kessler (eds.), p. 61
- Désert, F.-X., Boulanger, F., Puget, J.-L., 1990, A&A 237, 215
- Gabriel, C., Acosta-Pulido, J.A., 1999, Proc. "The Universe as seen by ISO", P. Cox & M. Kessler (eds.), p. 73
- Izumiura, H., Hashimoto, O., 1999, "Asymptotic Giant Branch Stars". T. Le Bertre, A. Lèbre & C. Waelkens (eds.), I.A.U. Symp. 191, p. 401
- Le Bertre, T., Lagache, G., Maunon, N., Boulanger, F., Désert, F.-X., Epchtein, N., Le Sidaner, P., 1998, A&A 335, 287
- Le Bertre, T., Maunon, N., Lagache, G., Boulanger, F., Désert, F.-X., Epchtein, N., Le Sidaner, P., 1999a, Proc. "The Universe as seen by ISO", P. Cox & M. Kessler (eds.), p. 361
- Le Bertre, T., Maunon, N., Lagache, G., Boulanger, F., Désert, F.-X., Epchtein, N., Le Sidaner, P., 1999b, "Atmospheres of M, S and C Giants". J. Hron & S. Höfner (eds.), p. 101
- Le Bertre, T., Winters, J.M., 1998, A&A 334, 173
- Le Sidaner, P., Le Bertre, T., 1996, A&A 314, 896
- Olofsson, H., Bergman, P., Eriksson, K., Gustafsson, B., 1996, A&A 311, 587
- Schulz, B., Huth, S., Kinkel, U., et al., 1999, Proc. "The Universe as seen by ISO", P. Cox & M. Kessler (eds.), p. 89